Stellar Rotation
Proceedings IAU Symposium No. 215, © 2003 IAU
André Maeder & Philippe Eenens, eds.

Measurements of Differential Rotation in Cool Stars

A. Reiners and J.H.M.M. Schmitt

Hamburger Sternwarte, Gojenbergsweg 112, D-21029 Hamburg

Abstract. We have obtained high resolution ($R \approx 220\,000$) - high signal-to-noise ($S/N > 500$) spectra of 142 field dwarfs of spectral types F–K and $v \sin i \leq 45\,\mathrm{km\,s^{-1}}$. Using the Fourier Transform Method (FTM) we precisely determined rotational velocities ($\Delta v \sin i < 1.0\ \mathrm{km\,s^{-1}}$). For stars with $v \sin i \geq 12.0\,\mathrm{km\,s^{-1}}$ this method allows the detection of deviations from solid body rotation. In the case of symmetric profiles the differential rotation parameter $\alpha = (\omega_{\mathrm{equator}} - \omega_{\mathrm{pole}}) / \omega_{\mathrm{equator}}$ can be determined. This was possible for 32 of our sample stars; ten stars show evidence for solar-like differential rotation with $\alpha > 0.0$. Thus it becomes possible to search for connections between differential rotation, rotational velocities and other stellar parameters. Signatures of differential rotation could be found on stars rotating as fast as $v \sin i = 42\,\mathrm{km\,s^{-1}}$. Particularly the Li-depleted stars turned out to show strong signatures of differential rotation. Our measurements support the idea, that Li-depletion in fast rotators ($v \sin i > 15\,\mathrm{km\,s^{-1}}$) is closely connected to differential rotation.

1. Introduction

Rotational line broadening is used as the main indicator for stellar rotational velocities. Regardless of the method used – e.g., measuring the line's FWHM or calculating $v \sin i$ from the zeros of the Fourier transform – the strategy is to measure the Doppler broadening proportional to the rotational velocity of the star. In case of not too fast rotators ($v \sin i < 100\,\mathrm{km\,s^{-1}}$), this method is shown to be reliable and rotational velocities can precisely be measured.

Modelling Doppler broadened absorption profiles in detail, a series of additional (turbulence) velocity fields have to be taken into account affecting the actual shape of the lines' profiles. Deviations between observed and modelled profiles can be studied if sufficiently high data quality (high resolution and high signal-to-noise ratio) is available. One of the effects known to cause deviations from standard rotation profiles is differential rotation and it is possible to search for such deviations in the shape of stellar line profiles.

Differential rotation itself is suspected to cause internal mixing probably leading to enhanced surface depletion of Li. On the other hand it is the underlying mechanism driving a stellar dynamo that is believed to be the ultimate cause of the plethora of stellar activity phenomena. Informations on differential rotation on stars other than the Sun will thus improve our understanding of stellar and solar interior and dynamo processes.

2. How to Measure Stellar Differential Rotation with FTM

Only very few information about stellar differential rotation exist and the only definite determination of differential rotation was made for the Sun. The solar rotation law can be approximated as

$$\omega(l) = \omega_0(1 - \alpha \sin^2 l), \tag{1}$$

with l the latitude, ω_0 the angular velocity at the equator and $\alpha_\odot \approx 0.2$ as measured from sunspots. In order to measure stellar differential rotation the rotation law of Eq. (1) is adopted and α is the parameter to be determined.

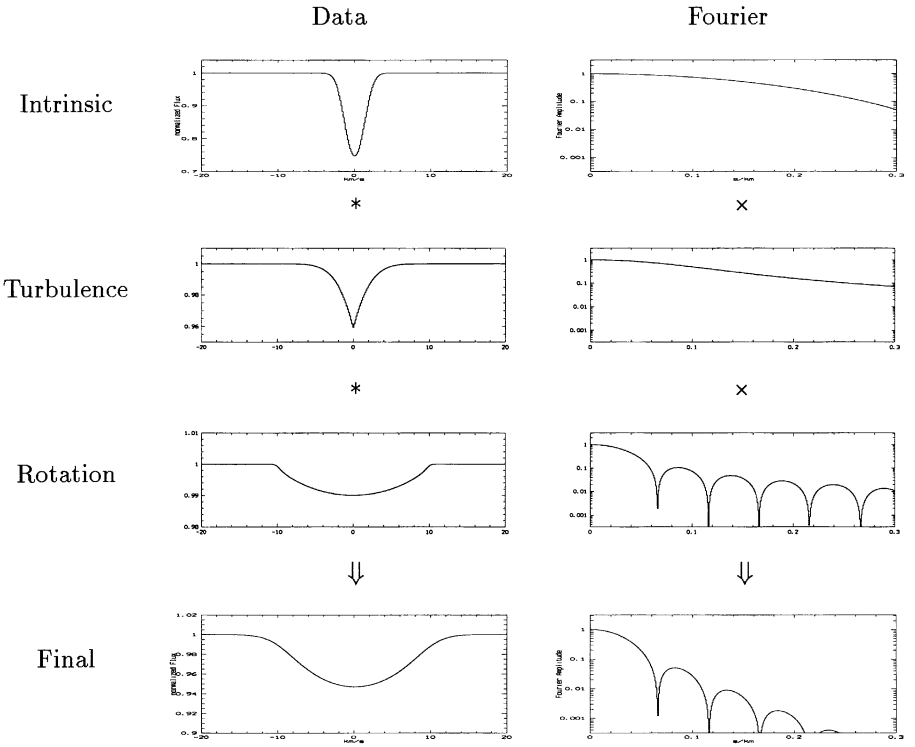

Figure 1. A stellar absorption line can be interpreted as a convolution of an intrinsic line profile with broadening profiles due to turbulence and rotation. The profiles are shown in data (left panel) and Fourier space (right panel). Since convolutions become multiplications in Fourier domain, zeros of the Fourier transformed rotational broadening profile are visible in the Fourier transformed final (observed) profile.

To determine the effect of rotation on the absorption line profiles, rotational broadening has to be disentangled from other broadening mechanisms like turbulent flows. As an approximation the net effect of the various broadening mechanisms can be interpreted as convolutions of the broadening profiles due

https://doi.org/10.1017/S0074180900195439 Published online by Cambridge University Press

to each of the velocity fields. In data space disentangling remains complicated, but since convolutions become multiplications in Fourier space, the situation improves using the Fourier transforms of the broadening profiles. In Fig. 1 the constituents of a typical broadening profile are shown in data and Fourier domain. The final line profile is a convolution ($*$) of the intrinsic absorption line convolved with a turbulence profile and the rotational broadening profile.

In Fourier domain the advantages of multiplication ($\times$) become apparent; for sufficiently fast rotating stars the only component possessing zeros is the rotational broadening profile. In high-quality spectra these zeros can directly be detected in the Fourier transform of the final profile.

Simulations (Reiners & Schmitt 2002a) showed that the first two zeros, q_1 and q_2, of the Fourier transform of rotational broadening profiles significantly depend on the parameter α used in Eq. (1) and on the inclination i under which a star is observed. In Fig. 2 this ratio q_2/q_1 is shown for a range of values of the parameters α and i; darker grey indicates smaller values of q_2/q_1. The ratio q_2/q_1 is an unambiguous indicator for solar-like differential rotation (positive α, equator faster than pole). The dependence of q_2/q_1 on both α and i only allows the determination of a combination of both parameters, the slope in Fig. 2 can be fitted using the parameter $\alpha/\sqrt{\sin i}$, which can thus directly be determined from the Fourier transform of an observed line profile.

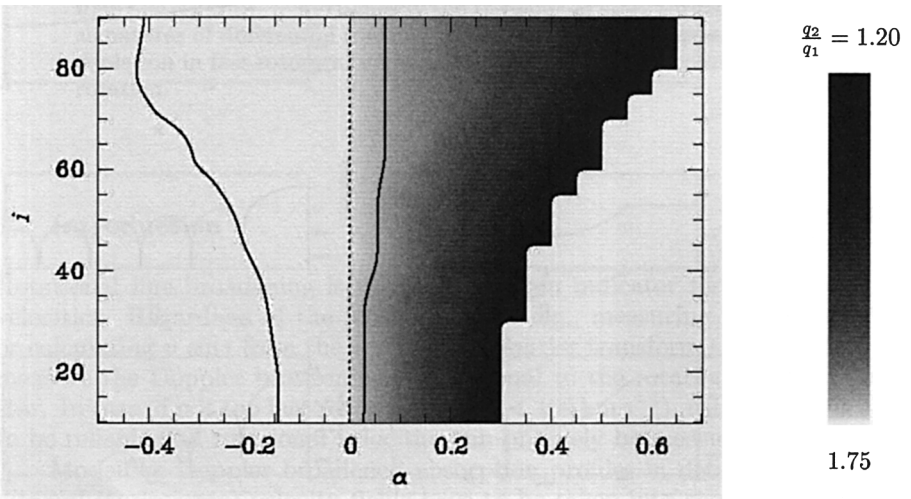

Figure 2. Dependence of q_2/q_1 – the ratio of the first two zeros of Fourier transformed rotational broadening profiles – on the differential rotation α and the inclination angle i. For solar-like differential rotation ($\alpha > 0$) q_2/q_1 depends monotonically on $\alpha/\sqrt{\sin i}$. The region between the solid lines around $\alpha = 0$ can be achieved with rigid rotation and extreme limb darkening.

3. Physical Least Squares Deconvolution

Broadening due to stellar velocity fields has identical effects on all absorption lines. The ideal strategy to search for effects of differential rotation is thus to

https://doi.org/10.1017/S0074180900195439 Published online by Cambridge University Press

derive an overall broadening profile from all observed spectral lines. Using a large amount of spectral lines enhances the signal-to-noise ratio and blending is properly accounted for simultaneously.

We thus used a "Physical Least Squares Deconvolution" (PLSD) method to derive an overall broadening profile from all identified spectral lines contained in our wavelength region. The details of the method should not be considered here and can be found in Reiners & Schmitt (2003). A typical result of the PLSD is shown in Fig. 3. An overall broadening profile (shown in the upper right panel) is calculated in order to achieve an optimal agreement between the observed spectrum and the convolution of the template (upper left panel) and this broadening profile. In the lower panel the achieved fit is plotted over the data's error bars. A difference to the data can hardly be found demonstrating the quality of the fit.

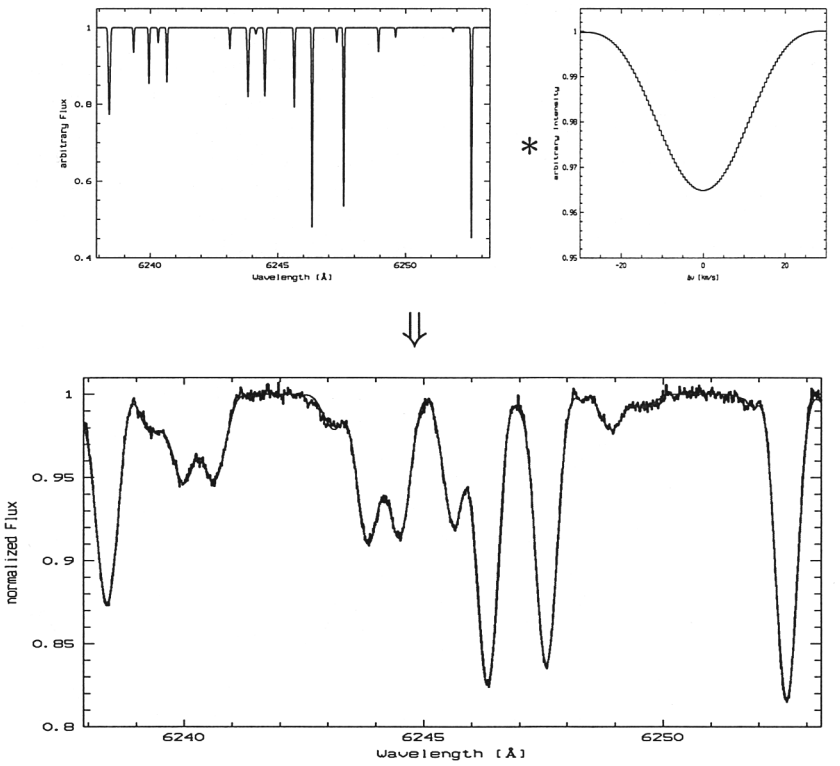

Figure 3. Example of a result of the Physical Least Squares Deconvolution. The physical (thermal broadened) template shown in the upper left figure is convolved with the achieved overall broadening profile (upper right). The result is plotted over the original data in the bottom panel.

https://doi.org/10.1017/S0074180900195439 Published online by Cambridge University Press

4. Observations

We obtained high quality spectra of 142 field stars of spectral type F–K with a resolution of $R \sim 220\,000$ and $S/N > 500$. Rotational velocities for these stars were determined from the zeros of the Fourier transforms with an accuracy better than $1.0\,\mathrm{km\,s^{-1}}$ in most cases. A complete list of our results can be found in Reiners & Schmitt (2003) or at the CDS. For stars with $v \sin i \geq 12\,\mathrm{km\,s^{-1}}$ a determination of $\alpha/\sqrt{\sin i}$ was possible if the broadening profile was not dominated by spots (for a discussion on the influence of spots on the determination of α, cf. Reiners & Schmitt 2002b). For 32 stars we determined the amount of differential rotation $\alpha/\sqrt{\sin i}$. For 22 of the 32 stars (68%), our results are consistent with rigid rotation ($\alpha = 0$), in the remaining ten stars we found significant evidence for solar-like differential rotation ($\alpha > 0$).

Two extreme cases with strong signatures of differential rotation are shown in Fig. 4. In the left panel the Fourier transform of the overall broadening profile is shown with the appropriate error bars. In the right panel small regions of the spectra are shown, the solid line indicates the result of the convolution of our template and our derived broadening profile. Overplotted with dashed lines are synthetic profiles according to rigid rotation with the same values of $v \sin i$ as derived for the respective stars. No optimization of the fit of the rigid rotator using different turbulence velocities have been tried, since the large discrepancy in the zeros in Fourier domain cannot be improved by changing the turbulence velocities. The only mechanism known shifting the zeros of the Fourier transform as strongly as observed (left panel) is solar-like differential rotation.

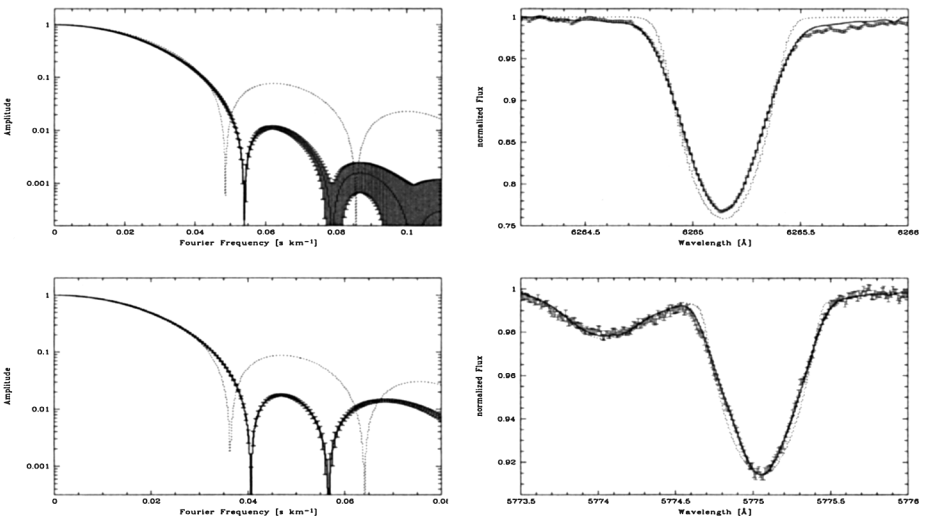

Figure 4. Two cases of strong differential rotation; HD 121 370 (top panel) and HD 173 667 (bottom panel). Left panel: Fourier transform of the derived overall broadening profile; right panel: data region. See text for details.

https://doi.org/10.1017/S0074180900195439 Published online by Cambridge University Press

5. Stellar Differential Rotation and Internal Mixing

In Fig. 5 the values of $\alpha/\sqrt{\sin i}$ are plotted against $v \sin i$ for the 32 cases where the determination was possible. Differential rotation appears to be more frequent for the slower rotating stars, but this may be due to the limited sample and selection effects during the analysis. Differential rotation was even found on a star rotating with a value of $v \sin i > 40\,\mathrm{km\,s^{-1}}$. For stars where measurements of Li abundance were available in the literature, the Li abundance is indicated with a symbol in Fig. 5; measurements marked with open circles are from stars with $\log \epsilon\,(\mathrm{Li}) > 1.7$, crosses indicate stars with $\log \epsilon\,(\mathrm{Li}) < 1.7$, the latter are essentially upper limits.

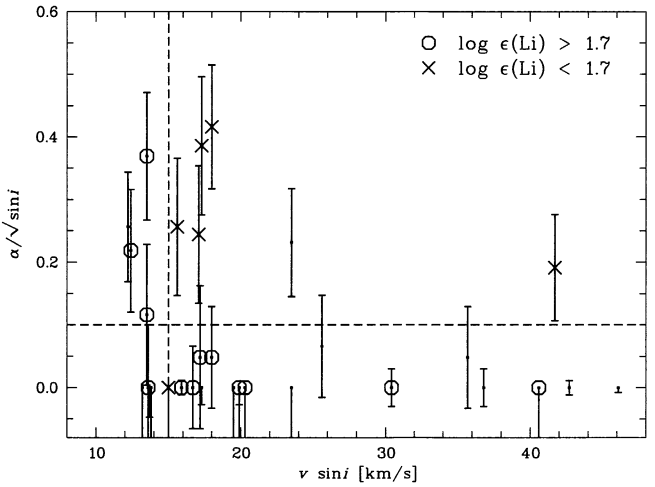

Figure 5. Differential rotation $\alpha/\sqrt{\sin i}$ vs. $v \sin i$ for the 32 stars where measurements were possible. Overplotted symbols indicate Li abundances. Fast ($v \sin i > 15\,\mathrm{km\,s^{-1}}$) differential rotators appear Li-depleted.

All stars rotating faster than $v \sin i = 15\,\mathrm{km\,s^{-1}}$ that show evidence for differential rotation (and for which values of Li abundances exist) appear to be Li-depleted (crosses), while all except one of the other objects have $\log \epsilon\,(\mathrm{Li}) > 1.7$. The single Li-depleted star with no signature of solar-like differential rotation has a remarkably slow value of q_2/q_1 probably indicating a polar spot (cf. Reiners & Schmitt 2002b). We thus conclude that differential rotation seems to be closely connected to Li-depletion in "fast" rotating ($v \sin i = 15\,\mathrm{km\,s^{-1}}$) solar-like stars indicating an internal mixing mechanism in these stars.

Acknowledgments. A.R. acknowledges financial support from Deutsche Forschungsgemeinschaft DFG-SCHM 1032/10-1.

References

Reiners A., Schmitt J.H.M.M., 2002a, A&A 384, 155
Reiners A., Schmitt J.H.M.M., 2002b, A&A 388, 1120
Reiners A., Schmitt J.H.M.M., 2003, A&A 398, 647